Nanoscale

RSC Publishing

PAPER

View Article Online
View Journal | View Issue



Cite this: *Nanoscale*, 2013, **5**, 4751

# Spin-polarized transport through single-molecule magnet $Mn_6$ complexes†

Eduard Cremades,[a] C. D. Pemmaraju,[b] Stefano Sanvito*[b] and Eliseo Ruiz*[a]

Received 4th January 2013
Accepted 22nd March 2013

DOI: 10.1039/c3nr00054k

www.rsc.org/nanoscale

The coherent transport properties of a device, constructed by sandwiching a $Mn_6$ single-molecule magnet between two gold surfaces, are studied theoretically by using the non-equilibrium Green's function approach combined with density functional theory. Two spin states of such $Mn_6$ complexes are explored, namely the ferromagnetically coupled configuration of the six $Mn^{III}$ cations, leading to the $S = 12$ ground state, and the low $S = 4$ spin state. For voltages up to 1 volt the $S = 12$ ground state shows a current one order of magnitude larger than that of the $S = 4$ state. Furthermore this is almost completely spin-polarized, since the $Mn_6$ frontier molecular orbitals for $S = 12$ belong to the same spin manifold. As such the high-anisotropy $Mn_6$ molecule appears as a promising candidate for implementing, at the single molecular level, both spin-switches and low-temperature spin-valves.

## Introduction

Over the past few years junctions based on individual molecules have emerged as a tantalizing strategy towards device down-scaling.[1,2] In particular junctions incorporating magnetic molecules can be exploited to control the spin of charge carriers, yielding to spin-dependent transport devices, such as spin valves.[3–5] Single-molecule magnets (SMM) are compounds with a relatively large magnetic anisotropy that allows fixing the spin direction even in the absence of an external magnetic field.[6–8] The magnitude of the magnetic anisotropy is the key physical parameter, because it controls the height of the spin-flip barrier $DS^2$, with $D$ being the axial zero-field splitting parameter and $S$ the total spin of the ground state. Thus, such systems can behave as individual nanomagnets. One has then to select, among the many, the best SMM to be incorporated into a junction. This is a difficult task because the properties of a SMM in the single crystal form may not be transferable to the same molecule deposited on a surface. For instance the widely studied $Mn_{12}$ family,[9,10] comprising many mixed valence $Mn^{III}$–$Mn^{IV}$ complexes, displays rather high instability when coordinated to metallic surfaces.[11,12] From the experimental point of view,[13] the transport properties of some SMMs have been explored in three-terminal devices; in particular $Mn_{12}$,[14,15] $Mn_4$,[16] $Fe_4$ (ref. 17–19) and single-ion magnet bis-phthalocyaninato $Tb^{III}$ complex[20–23] have all been used to make spin-molecular-devices. Here we consider a different family of molecules, namely the $Mn_6$ complexes.[24] These have some advantages with respect to other SMMs: (i) all the cations are $Mn^{III}$, thus we expect an electrochemical stability larger than that of mixed-valence systems, (ii) some of the $Mn_6$ are SMMs with the record magnetic anisotropy barrier for complexes containing first-row transition metals,[25–27] (iii) small structural changes lead to a crossover from the $S = 12$ to the $S = 4$ ground state[28,29] and (iv) the electronic structure for the $S = 12$ ground state corresponds to a parallel spin alignment of all the Mn ions.

From the theoretical point of view, the usual approach to study coherent transport properties in these kinds of systems is that of employing electronic structure calculations,[30,31] usually based on density functional theory (DFT), combined with the non-equilibrium Green's function (NEGF) method for electron transport.[32,33] For instance such an approach was previously employed to study electron transport in junctions incorporating $Mn_{12}$ SMMs.[34–39] DFT methods can also be applied to calculate the zero field splitting parameters that quantify the magnetic anisotropy of such molecules.[40–43] Ruiz *et al.* have investigated magnetic anisotropy for the two $S = 12$ to the $S = 4$ ground states of some $Mn_6$ complexes.[44] The main goal of this work is to compare the transport mechanism across $Mn_6$ SMM complexes sandwiched between two gold surfaces, when the molecule switches between the $S = 12$ and the $S = 4$ ground states. Due to the small exchange coupling constants present in such systems, there is a small energy difference between the two states,[45] of around 44 $cm^{-1}$.[28] This opens the possibility of switching between the different spin-states by using some external

[a]*Departament de Química Inorgànica and Centre de Recerca en Química Teòrica, Universitat de Barcelona, Diagonal 645, 08028 Barcelona, Spain. E-mail: eliseo.ruiz@qi.ub.es*

[b]*School of Physics and CRANN, Trinity College, Dublin 2, Ireland*

† Electronic supplementary information (ESI) available: Calculated total and projected density of states of an isolated $[Mn_6O_2(Et\text{-}sao)_6\{O_2CPh(Me)_2\}_2(EtOH)_6]$ original SMM complex (Fig. S1). Calculated total and projected density of states of an isolated $[Mn_6O_2(Me\text{-}sao)_6\{O_2CPh(SH)\}_2(MeOH)_6]$ model complex (Fig. S2). Transmission spectra calculated at different voltages corresponding to the $S = 12$ and $S = 4$ ground states for the $Mn_6$–Au(111) layer system (Fig. S3). Cell parameters and Cartesian coordinates of the $Mn_6$–Au(111) layer system. See DOI: 10.1039/c3nr00054k

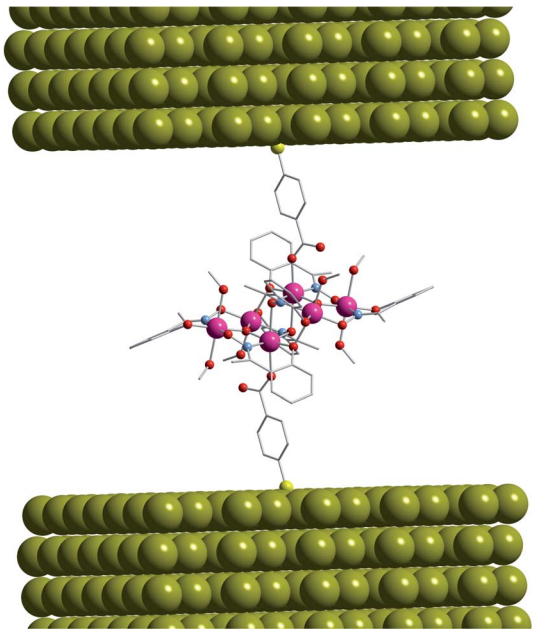

**Fig. 1** Model structure of a $[Mn_6O_2(Me\text{-}sao)_6\{O_2CPh(SH)\}_2(MeOH)_6]$ molecule coordinated to five layers of the Au(111) with the S-atoms located in 3-fold hollow sites (S–Au plane distance of 2.1 Å). Pink, yellow, red and blue spheres correspond to manganese, sulfur, oxygen and nitrogen atoms, respectively, while the carbon atoms are represented as a grey wire.

stimuli. Intriguingly, Prescimone *et al.* showed that under pressure, it is possible to modify the relative energies of the states of some $Mn_6$ complexes.[46] Under a pressure of 17.5 kbar, the energy difference between the ground state ($S = 12$) and the first excited state ($S = 11$) is reduced more than 80%. Recently, Timm and Di Ventra have theoretically proposed that single-molecule magnets coupled to ferromagnetic leads will have memristor properties.[47]

The family of $Mn_6$ complexes is now one of the most prolific complexes in the field of SMMs.[24] The basic structure can be described as two $Mn_3O$ triangles with equatorial oximato and axial carboxylate bridging ligands (see Fig. 1). Many different carboxylate ligands have been employed but the magnetic properties are mainly controlled by the equatorial oximato bridging ones. Thus, ferromagnetic coupling is found for the intra-triangle exchange interactions if the Mn–N–O–Mn angle is larger than a magic angle of around 30°, while antiferromagnetism appears for smaller torsions.[25] This magnetostructural correlation as well as the magnetic anisotropy in this family of complexes have been analysed in the past by some of us using DFT methods.[27,28] If the $Mn_6$ complexes have a small Mn–N–O–Mn angle in the $Mn_3O$ triangles, the coupling is antiferromagnetic resulting in a $S = 2$ ground state for each of the $Mn_3O$ triangles. As the inter-triangle exchange interactions are ferromagnetic, one finds a total spin $S = 4$ for the entire $Mn_6$ molecule.

## Results and discussion

In order to study the transport properties, we have selected the $S = 12$ $[Mn_6O_2(Et\text{-}sao)_6\{O_2CPh(Me)_2\}_2(EtOH)_6]$ structure, which shows the current record anisotropy for polynuclear complexes with first-row transition metals.[25,26] We then add two thiol groups to graft the molecule between the two Au(111) surfaces and replace both the ethyl groups of the equatorial sao oximato and the ethanol ligands with methyl. This reduces the size of the system (see Fig. 1), and hence the calculation, without affecting the electronic structure relevant for the transport. Moro *et al.* have grafted some $Mn_6$ complexes to Au(111) surfaces through thiophene carboxylate ligands and showed by X-ray photoemission spectroscopy that the core stoichiometry and the $Mn^{III}$ oxidation state remain preserved.[48,49] Del Pennino *et al.* performed some LDA+*U* calculations for a monolayer of $Mn_6$ SMM grafted onto Au(111) to compare the calculated density of states with the experimental spectroscopic data.[50]

For isolated $Mn_6$ molecules we have performed DFT calculations with the Ceperley–Alder parameterization[51] of the local density approximation (LDA) functional by using the SIESTA code.[52–54] Then transport simulations are carried out by including self-interaction correction (ASIC)[55,56] as implemented in the SMEAGOL code.[3,57] The ASIC functional generally improves the molecule fundamental gap and, as a consequence, usually offers a better description of the transport properties[58] (see more detailed information in the Computational details section). The density of states (DOS) for the $S = 12$ and $S = 4$ ground states of the original complex $[Mn_6O_2(Et\text{-}sao)_6\{O_2CPh(Me)_2\}_2(EtOH)_6]$ and the model complex employed for the transport calculation have been thoroughly compared (see ESI Fig. S1 and S2†), showing almost identical features. This justifies the use of the smaller molecule in the transport calculations. The $S = 4$ ground state corresponds to the spin flipping of two of the central $Mn^{III}$ cations.[28] As expected, the HOMO and LUMO orbitals receive predominant contributions from the Mn d orbitals with a small mixing of 2p ones of the O, C and N atoms of the ligands.

The local electronic structure of the $Mn^{III}$ cations is modulated by a Jahn–Teller effect that induces long axial distortion resulting in the splitting of the $e_g$ levels, with energy stabilization of $d_{z^2}$ orbital while the $d_{x^2-y^2}$ one remains empty. In Fig. 2, we present the DOS and the zero-bias transmission spectra for the $S = 12$ ground state of the $Mn_6$–Au(111) junction. In this case the parallel alignment of all the spins is reflected in the fact that the $Mn_6$ DOS contribution close to the Fermi level presents only the alpha spin direction. Thus, all the first occupied molecular orbitals going from the HOMO-5 to the HOMO (see Fig. 2) are mainly due to the six combinations of the $d_{z^2}$ orbitals of the $Mn^{III}$ cations. The HOMO and HOMO-1 receive major contributions from the central $Mn^{III}$ cations and correspond to the highest transmission peaks. The HOMO-2 and HOMO-3 are centred on the external manganese atoms of one of the two $Mn_3O$ triangles. Finally, the two similar HOMO-4 and HOMO-5 are delocalized on the six $Mn^{III}$ cations showing a mixing of the $d_{z^2}$ orbital with some $t_{2g}$ ones. The six combinations of the $d_{x^2-y^2}$ orbitals form the first empty orbitals and they appear in the form of three pairs. The LUMO and the similar LUMO+1 levels are a combination of the $d_{x^2-y^2}$ orbitals with a similar contribution from the six $Mn^{III}$ cations and the 2s orbital of the central oxygen atom. In the LUMO, the orbitals belonging to the

 

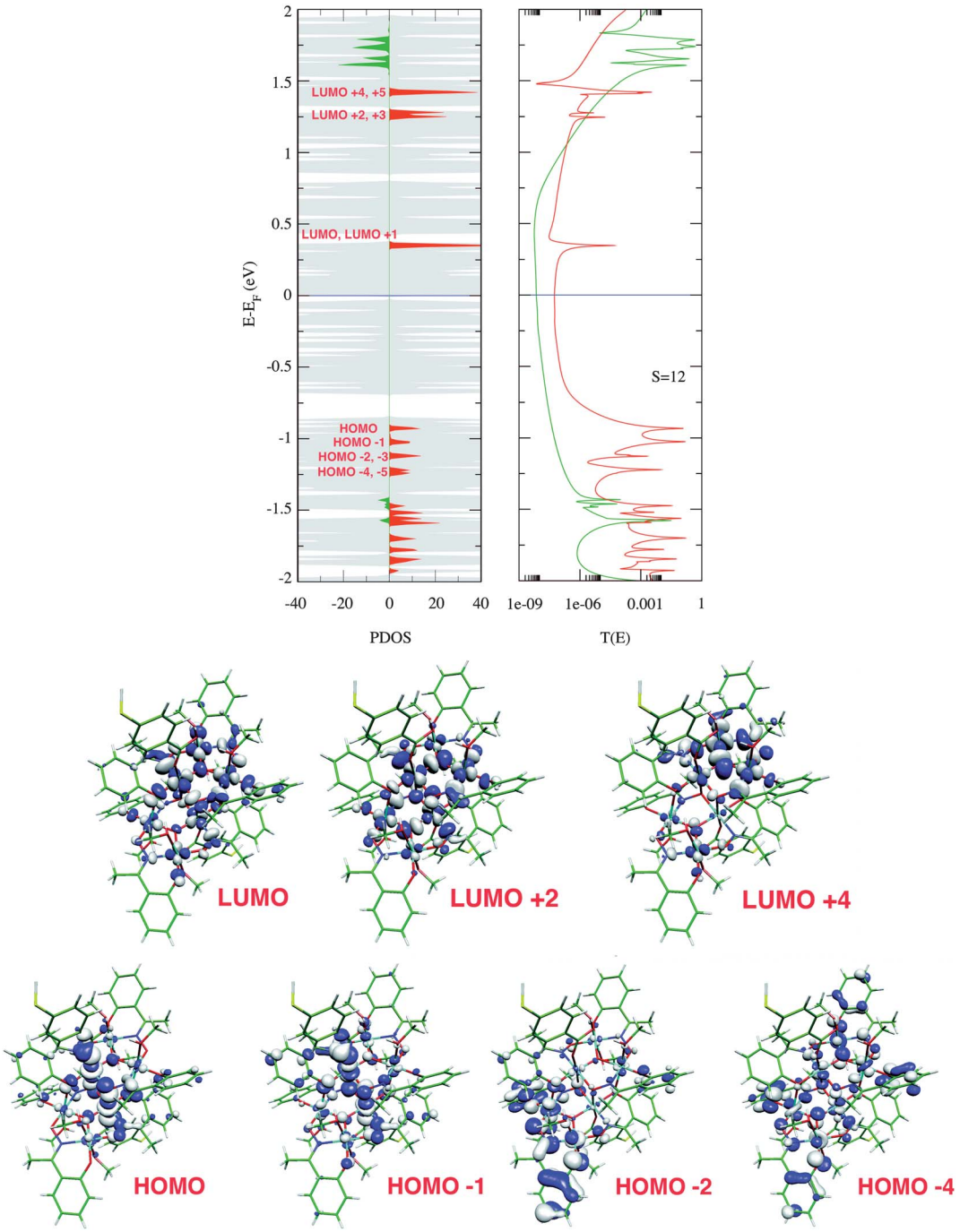


**Fig. 2** Projected density of states (PDOS) and zero-bias transmission spectra, $T(E)$, of the Au(111)–$Mn_6$–Au(111) junction with the molecule in the $S = 12$ spin state. Red and green PDOS correspond to the alpha and beta projections over the manganese atoms, while the contribution from the gold atoms is shown in grey. In the lower panel we present isosurfaces of the electron wavefunction of the most significant molecular orbitals.

two $Mn_3O$ triangles are in-phase while the LUMO+1 corresponds to the out-of-phase combination. The LUMO+2 and LUMO+3 states also have contribution from the six manganese atoms but now they are mixed with a 2p orbital of the central oxygen. Finally the LUMO+4 and LUMO+5 are mainly confined over one of the two $Mn_3O$ triangles. The transmission coefficient as a function of energy, $T(E)$, nicely reflects the position of the various peaks in the DOS, *i.e.* there is a transmission resonance at any energy corresponding to a molecular level. The height and the width of such resonances depend on the electronic coupling between the particular molecular level and the electrodes and it is ultimately determined by the symmetry of the given level. In this case, however, the Fermi level of the electrodes lies well within the HOMO–LUMO gap, meaning that the transport is tunnelling in nature. As a consequence the transmission at the Fermi level, which determines the low-bias conductance, depends on the tail of the transmission resonances closer to $E_F$. We then find that $T(E_F)$ for the alpha

electrons is much larger than that for the beta, so that the low-bias conductance is almost entirely spin-polarized.

Let us now move to the $S = 4$ case, whose DOS and zero-bias transmission spectra are shown in Fig. 3. Now the beta HOMO and HOMO-1 levels are a combination of $d_{z^2}$ orbitals belonging to the two central $Mn^{III}$ cations, while the corresponding alpha orbitals are a combination of $d_{z^2}$ orbitals centred on the other four $Mn^{III}$ cations (alpha orbitals from HOMO to HOMO-3). The occupied beta HOMO and HOMO-1 levels present higher transmission peaks and are also closer to the Fermi level than the corresponding alpha orbitals. The beta LUMO, also closer to the Fermi level than the alpha one, is a combination of the $d_{x^2-y^2}$ state of the central spin-down $Mn^{III}$ cations. The alpha HOMO and HOMO-1 orbitals are mainly centred on the external Mn atoms of one of the $Mn_3O$ triangles. Finally the alpha HOMO-2 and HOMO-3 show contribution from the four external $Mn^{III}$ cations. When the molecule is in the $S = 4$ spin state the HOMO–LUMO gaps of the different spin manifolds are much more similar to each other than in the $S = 12$ case. This fact, combined with the different orbital symmetries of the spin-split frontier molecular orbitals, yields almost identical transmission coefficients at the Fermi level for the two spin species. As a

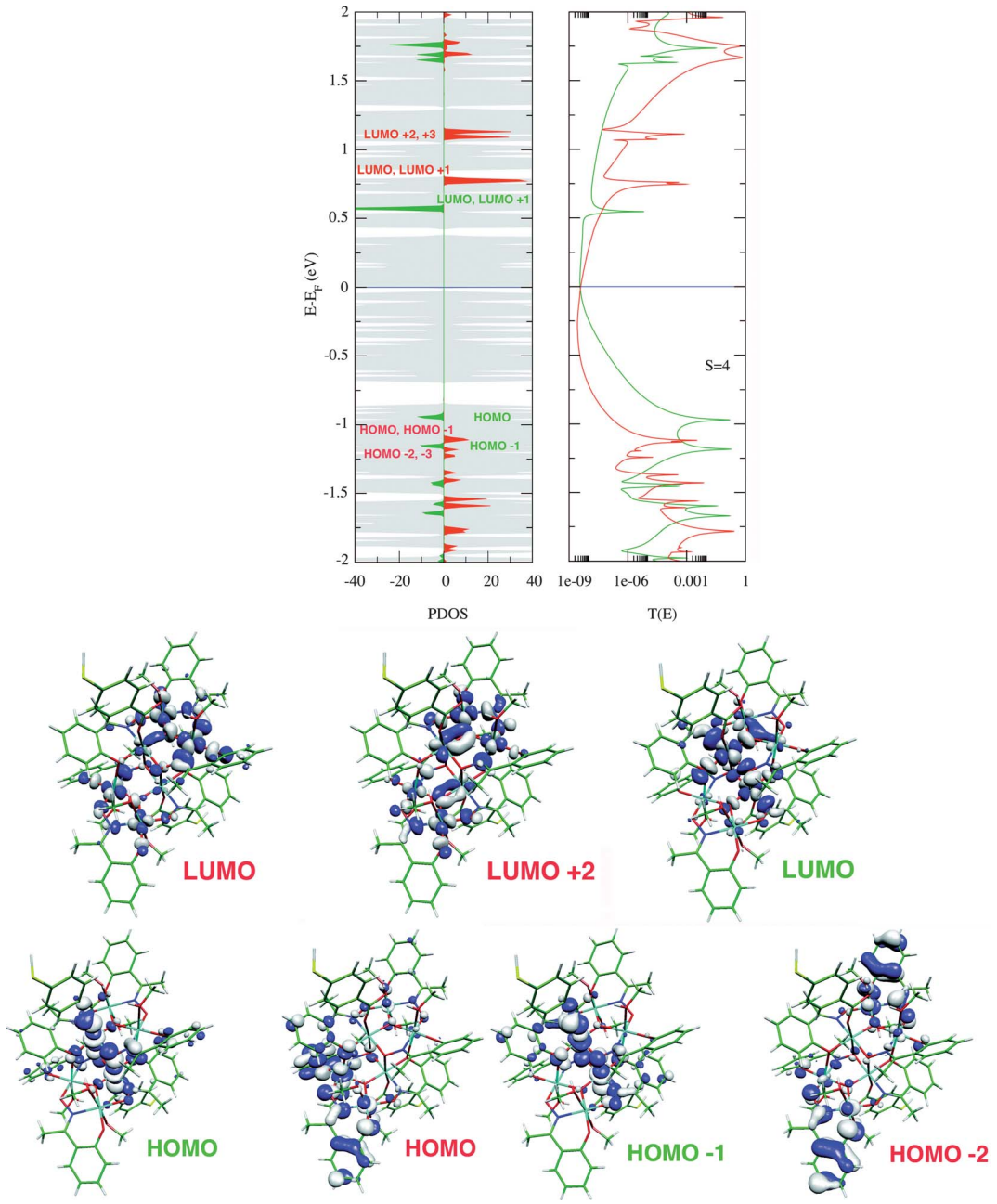


**Fig. 3** Projected density of states (PDOS) and zero-bias transmission spectra, $T(E)$, of the Au(111)–$Mn_6$–Au(111) junction with the molecule in the $S = 4$ spin state. Red and green PDOS correspond to the alpha and beta projections over the manganese atoms, while the contribution from the gold atoms is shown in grey. In the lower panel we present isosurfaces of the electron wavefunction of the most significant molecular orbitals.

 

consequence the current at low-bias is expected to be almost spin-degenerate. Concerning the possibility of redox molecular processes and the presence of Coulomb blockade peaks, a rough estimate can be provided by the distance between the Fermi level and the HOMO or LUMO, which is always around 0.5 eV, thus, up to 1 V no Coulomb blockade peaks are expected. Theoretical analysis of how the electronic properties are affected by redox processes has been previously reported by Park and Pederson[59] for $Mn_{12}$ complexes and Canali and coworkers have studied the transport properties of such single-molecule magnet complexes.[37,60]

We finally move on to discuss the transport properties of the junction at finite bias. The calculated *I–V* curves for the different spin states and their spin-resolved contributions are presented in Fig. 4. These are obtained by performing an energy integration of the spin and bias-dependent transmission coefficients over the bias window (see Fig. S3 in ESI†). In actual fact $T(E)$ does not change much with bias for the bias range investigated here, with the exception of a small split of the LUMO-related peak for both the spin states. As such, the integration of the zero-bias $T(E)$ provides already a good rationale for the *I–V* curves. We note that there are dramatic differences between the *I–V* curves of the two spin states: (i) the $S = 12$ ground state shows a much larger current at all voltages, almost one order of magnitude larger than that of the $S = 4$ state; (ii) since for the $S = 12$ ground state the electronic structure of the $Mn^{III}$ cations presents only alpha orbitals close to the Fermi level (see Fig. 2), the current is almost perfectly spin polarized, being the conduction of the beta electrons practically negligible; (iii) for the $S = 4$ state the conduction is mainly due to the beta electrons but there is a similar alpha contribution at low bias values (recall that $T(E_F)$ is essentially the same for the two spins, see Fig. 3). Most of these results can be attributed to the position of the LUMO and LUMO+1 orbitals in the two cases. In fact the LUMO/LUMO+1 of the $S = 12$ ground state is 0.25 eV closer to the Fermi level of the electrodes than that of the $S = 4$ state, while the corresponding HOMOs are approximately in the same position. As such the differences in transport properties are mainly due to a difference in band-gap between the two spin states.

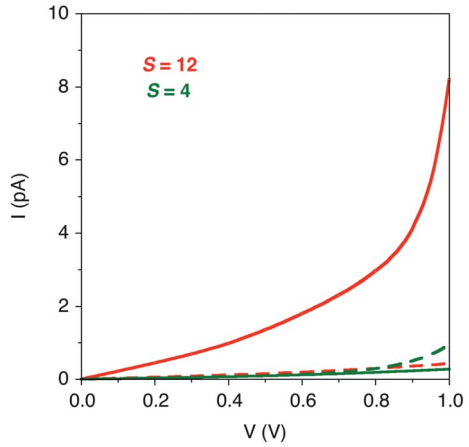


**Fig. 4** *I–V* characteristics for the Au(111)–$Mn_6$–Au(111) junction when the molecule is either in the $S = 12$ (red line) or $S = 4$ (green line) spin state. The solid and dashed curves correspond to the contributions to the current from the alpha and beta electrons, respectively.

## Conclusions

We have demonstrated that the transport properties of $Mn_6$ SMM complexes immobilized inside a two-terminal junction depend sensitively on the molecule spin state. Two different spin states of such $Mn_6$ complexes have been explored, the $S = 12$ ferromagnetically coupled state with a parallel alignment of the spin of the six $Mn^{III}$ cations and the low $S = 4$ spin configuration corresponding to the inversion of one of the $Mn^{III}$ cations of each $Mn_3$ triangle. For voltages up to 1 volt the $S = 12$ ground state shows a current one order of magnitude larger than that of the $S = 4$ state. For such voltages we should expect that the molecule would keep the original neutral state without redox processes and consequently, the Coulomb blockade mechanism is not expected. Moreover this is almost completely spin-polarized, since the $Mn_6$ frontier molecular orbitals for $S = 12$ belong to the same spin manifold. This is similar to what was found both experimentally[61–63] and theoretically[64,65] for spin-crossover compounds based on $Fe^{II}$. Also, $Co^{II}$ dioxolene valence tautomeric complexes have been proposed for similar application due to switching between the $Co^{II}$-semiquinone and $Co^{III}$-catechol species.[66,67] Intriguingly, at variance with the mononuclear $Fe^{II}$ or $Co^{II}$ complexes, the $Mn_6$ family may also display large magnetic anisotropy, which can be in principle probed by magnetic electrodes. As such the $Mn_6$ family appears as an intriguing material platform for both low-temperature molecular spin-valves and spin-switches.

## Computational details

The SIESTA code,[52–54] which is based on numerical orbital basis sets and norm-conserving pseudopotentials, was employed to perform calculations of the density of states of isolated $Mn_6$ molecules. Transport calculations were performed using the experimental X-ray structure of $[Mn_6O_2(Et\text{-}sao)_6\{O_2CPh(Me)_2\}_2(EtOH)_6]$ including the structural changes described above. The LDA functional proposed by Ceperley and Alder[51] was employed with a self-interaction correction (ASIC).[55,56] The inclusion of the ASIC considerably improves one of the main deficiencies of DFT. The self-interaction error[68–70] causes a wrong asymptotic behavior of the functional and the energy gaps are underestimated.[71–73] Thus, the ASIC approach gives a more appropriate description of the energy levels that is crucial for the proper prediction of transport properties.

We employed scalar relativistic pseudopotentials with the following reference configurations: H $1s^1$, C $2s^22p^2$, S $3s^23p^4$, O $2s^22p^4$, Mn $4s^23d^5$ and Au $6s^1$. The atomic basis sets were the following: H: DZP-s; C: DZ-s, DZ-p; S: DZ-s, DZP-p, SZ-d; O: DZ-s, DZP-p, SZ-d; Mn: DZP-s, SZP-p, DZ-d and Au: DZ-s. It is worth noting that for atoms, the Au 5d orbitals were not directly considered resulting in a considerable reduction of computer time. This approximation was previously tested providing satisfactory results for transport properties.[58]

Transport calculations were performed using the SMEAGOL program[3,57] that combines the non-equilibrium Green's function approach[32,33] with the DFT calculations implemented in the SIESTA code. The charge density is calculated by splitting the integral of the Green's function into a contribution obtained over the complex energy plane and one along the real axis. The complex integral is carried out on a mesh of 512 imaginary energies while the real part is obtained using a mesh refinement algorithm to integrate the DOS peaks. The integration of the non-equilibrium density in a 2 eV bias window is performed including 10 000 energy points with a denser energy spacing being around $10^{-7}$ eV.

Calculations were performed for two spin configurations, the $S = 12$ and one $S = 4$ corresponding to the spin inversion of one $Mn^{III}$ center of each $Mn_3$ triangle. We have calculated the most stable $S = 4$ spin configuration and it corresponds to the spin inversion of one of the central $Mn^{III}$ centers (major contribution of the beta HOMO orbital in Fig. 3).

## Acknowledgements

The research has been supported by the *Ministerio de Ciencia e Innovación* and *Generalitat de Catalunya* through grants CTQ2011-23862-C02-01 and 2009SGR-1459, respectively. E. C. thanks *Ministerio de Ciencia e Innovación* for a predoctoral fellowship and for funding his stay in Dublin. C. D. P. and S. S. thank additional funding support from Science Foundation of Ireland (grant no. 07/IN/I945), by KAUST (FIC/2010/08) and by CRANN. The authors thankfully acknowledge the computer resources, technical expertise and assistance provided by the Barcelona Supercomputer Center.

## References

1 R. M. Metzger, *J. Mater. Chem.*, 2008, **18**, 4364.
2 J. C. Cuevas and E. Scheer, *Molecular Electronics: An Introduction to Theory and Experiment*, World Scientific Publishing Company, Singapore, 2010.
3 A. R. Rocha, V. G. Suarez, S. W. Bailey, C. J. Lambert, J. Ferrer and S. Sanvito, *Nat. Mater.*, 2005, **4**, 335.
4 S. Sanvito, *Chem. Soc. Rev.*, 2011, **40**, 3336.
5 L. Bogani and W. Wernsdorfer, *Nat. Mater.*, 2008, **7**, 179.
6 D. Gatteschi and R. Sessoli, *Angew. Chem., Int. Ed.*, 2003, **42**, 268.
7 D. Gatteschi, R. Sessoli and J. Villain, *Molecular Nanomagnets*, Oxford University Press, Oxford, 2006.
8 J. R. Friedman and M. P. Sarachik, *Annu. Rev. Condens. Matter Phys.*, 2010, **1**, 109.
9 R. Bagai and G. Christou, *Chem. Soc. Rev.*, 2009, **38**, 1011.
10 R. Sessoli, D. Gatteschi, A. Caneschi and M. A. Novak, *Nature*, 1993, **365**, 141.
11 A. Cornia, A. C. Fabretti, M. Pacchioni, L. Zobbi, D. Bonacchi, A. Caneschi, D. Gatteschi, R. Biagi, U. Del Pennino, V. De Renzi, L. Gurevich and H. S. J. Van der Zant, *Angew. Chem., Int. Ed.*, 2003, **42**, 1645.
12 A. Cornia, M. Mannini, P. Sainctavit and R. Sessoli, *Chem. Soc. Rev.*, 2011, **40**, 3076.
13 N. Crivillers, M. Mas-Torrent, C. Rovira and J. Veciana, *J. Mater. Chem.*, 2012, **22**, 13883.
14 H. B. Heersche, Z. de Groot, J. A. Folk, H. S. J. van der Zant, C. Romeike, M. R. Wegewijs, L. Zobbi, D. Barreca, E. Tondello and A. Cornia, *Phys. Rev. Lett.*, 2006, **96**, 206801.
15 M. Jo, J. E. Grose, K. Baheti, M. M. Deshmukh, J. J. Sokol, E. M. Rumberger, D. N. Hendrickson, J. R. Long, H. Park and D. C. Ralph, *Nano Lett.*, 2006, **6**, 2014.
16 F. Haque, M. Langhirt, E. del Barco, T. Taguchi and G. Christou, *J. Appl. Phys.*, 2011, **109**, 07B112.
17 M. Mannini, F. Pineider, C. Danieli, F. Totti, L. Sorace, P. Sainctavit, M. A. Arrio, E. Otero, L. Joly, J. C. Cezar, A. Cornia and R. Sessoli, *Nature*, 2010, **468**, 417.
18 M. Mannini, F. Pineider, P. Sainctavit, C. Denieli, E. Otero, C. Sciancalepore, A. M. Talarico, M. A. Arrio, A. Cornia, D. Gatteschi and R. Sessoli, *Nat. Mater.*, 2009, **8**, 194.
19 A. S. Zyazin, J. W. G. van den Berg, E. A. Osorio, H. S. J. van der Zant, N. P. Konstantinidis, M. Leijnse, M. R. Wegewijs, F. May, W. Hofstetter, C. Danieli and A. Cornia, *Nano Lett.*, 2010, **10**, 3307.
20 K. Katoh, H. Isshiki, T. Komeda and M. Yamashita, *Chem.–Asian J.*, 2012, **7**, 1154.
21 K. Katoh, H. Isshiki, T. Komeda and M. Yamashita, *Coord. Chem. Rev.*, 2011, **255**, 2124.
22 T. Komeda, H. Isshiki, J. Liu, Y.-F. Zhang, N. Lorente, K. Katoh, B. K. Breedlove and M. Yamashita, *Nat. Commun.*, 2011, **2**, 217.
23 R. Robles, N. Lorente, H. Isshiki, J. Liu, K. Katoh, B. K. Breedlove, M. Yamashita and T. Komeda, *Nano Lett.*, 2012, **12**, 3609.
24 R. Inglis, C. J. Milios, L. F. Jones, S. Piligkos and E. K. Brechin, *Chem. Commun.*, 2012, **48**, 181.
25 C. J. Milios, R. Inglis, A. Vinslava, R. Bagai, W. Wernsdorfer, S. Parsons, S. P. Perlepes, G. Christou and E. K. Brechin, *J. Am. Chem. Soc.*, 2007, **129**, 12505.
26 C. J. Milios, A. Vinslava, W. Wernsdorfer, S. Moggach, S. Parsons, S. P. Perlepes, G. Christou and E. K. Brechin, *J. Am. Chem. Soc.*, 2007, **129**, 2754.
27 A.-R. Tomsa, J. Martinez-Lillo, Y. Li, L.-M. Chamoreau, K. Boubekeur, F. Farias, M. A. Novak, E. Cremades, E. Ruiz, A. Proust, M. Verdaguer and P. Gouzerh, *Chem. Commun.*, 2010, **46**, 5106.
28 E. Cremades, J. Cano, E. Ruiz, G. Rajaraman, C. J. Milios and E. K. Brechin, *Inorg. Chem.*, 2009, **48**, 8012.
29 E. Cremades, T. Cauchy, J. Cano and E. Ruiz, *Dalton Trans.*, 2009, 5873.
30 N. A. Zimbovskaya and M. R. Pederson, *Phys. Rep.*, 2011, **509**, 1.
31 W. Y. Kim, Y. C. Choi, S. K. Min, Y. Cho and K. S. Kim, *Chem. Soc. Rev.*, 2009, **38**, 2319.
32 C. Caroli, R. Combescot, P. Nozieres and D. Saint-James, *J. Phys. C Solid State Phys.*, 1972, **5**, 21.
33 S. Datta, *Electronic Transport in Mesoscopic Systems*, Cambridge University Press, Cambridge, UK, 1995.
34 C. D. Pemmaraju, I. Rungger and S. Sanvito, *Phys. Rev. B: Condens. Matter Mater. Phys.*, 2009, **80**, 104422.

 

35 S. Barraza-Lopez, K. Park, V. García-Suárez and J. Ferrer, *J. Appl. Phys.*, 2009, **105**, 07E309.
36 S. Barraza-Lopez, K. Park, V. Garcia-Suarez and J. Ferrer, *Phys. Rev. Lett.*, 2009, **102**, 246801.
37 L. Michalak, C. M. Canali, M. R. Pederson, M. Paulsson and V. G. Benza, *Phys. Rev. Lett.*, 2010, **104**, 017202.
38 K. Park, S. Barraza-Lopez, V. M. Garcia-Suarez and J. Ferrer, *Phys. Rev. B: Condens. Matter Mater. Phys.*, 2010, **81**, 125447.
39 F. R. Renani and G. Kirczenow, *Phys. Rev. B: Condens. Matter Mater. Phys.*, 2012, **85**, 245415.
40 M. R. Pederson and S. N. Khanna, *Phys. Rev. B: Condens. Matter Mater. Phys.*, 1999, **60**, 9566.
41 F. Neese, *J.Chem. Phys.*, 2007, **127**, 164112.
42 S. Schmitt, P. Jost and C. van Wullen, *J. Chem. Phys.*, 2011, **134**, 194113.
43 C. van Wullen, *J. Chem. Phys.*, 2009, **130**, 194109.
44 E. Ruiz, J. Cirera, J. Cano, S. Alvarez, C. Loose and J. Kortus, *Chem. Commun.*, 2008, 52.
45 S. Carretta, T. Guidi, P. Santini, G. Amoretti, O. Pieper, B. Lake, J. van Slageren, F. El Hallak, W. Wernsdorfer, H. Mutka, M. Russina, C. J. Milios and E. K. Brechin, *Phys. Rev. Lett.*, 2008, **100**, 157203.
46 A. Prescimone, C. J. Milios, S. Moggach, J. E. Warren, A. R. Lennie, J. Sanchez-Benitez, K. Kamenev, R. Bircher, M. Murrie, S. Parsons and E. K. Brechin, *Angew. Chem., Int. Ed.*, 2008, **47**, 2828.
47 C. Timm and V. M. Di Ventra, *Phys. Rev. B: Condens. Matter Mater. Phys.*, 2012, **86**, 104427.
48 F. Moro, V. Corradini, M. Evangelisti, V. De Renzi, R. Biagi, U. del Pennino, C. J. Milios, L. F. Jones and E. K. Brechin, *J. Phys. Chem. B*, 2008, **112**, 9729.
49 F. Moro, V. Corradini, M. Evangelisti, R. Biagi, V. De Renzi, U. del Pennino, J. C. Cezar, R. Inglis, C. J. Milios and E. K. Brechin, *Nanoscale*, 2010, **2**, 2698.
50 U. del Pennino, V. Corradini, R. Biagi, V. De Renzi, F. Moro, D. W. Boukhvalov, G. Panaccione, M. Hochstrasser, C. Carbone, C. J. Milios and E. K. Brechin, *Phys. Rev. B: Condens. Matter Mater. Phys.*, 2008, **77**, 085419.
51 D. M. Ceperley and B. J. Alder, *Phys. Rev. Lett.*, 1980, **45**, 566.
52 E. Artacho, E. Anglada, O. Dieguez, J. D. Gale, A. Garcia, J. Junquera, R. M. Martin, P. Ordejon, J. M. Pruneda, D. Sanchez-Portal and J. M. Soler, *J. Phys.: Condens. Matter*, 2008, **20**, 064208.
53 E. Artacho, J. D. Gale, A. García, J. Junquera, R. M. Martin, P. Ordejón, D. Sánchez-Portal and J. M. Soler, *Siesta code v. 2.0*, Madrid, 2006.
54 J. M. Soler, E. Artacho, J. D. Gale, A. García, J. Junquera, P. Ordejón and D. Sánchez-Portal, *J. Phys.: Condens. Matter*, 2002, **14**, 2745.
55 C. Toher, A. Filippetti, S. Sanvito and K. Burke, *Phys. Rev. Lett.*, 2005, **95**, 146402.
56 C. D. Pemmaraju, T. Archer, D. Sánchez-Portal and S. Sanvito, *Phys. Rev. B: Condens. Matter Mater. Phys.*, 2007, **75**, 045101.
57 A. R. Rocha, V. García-Suárez, S. W. Bailey, C. J. Lambert, J. Ferrer and S. Sanvito, *Phys. Rev. B: Condens. Matter Mater. Phys.*, 2006, **73**, 085414.
58 C. Toher and S. Sanvito, *Phys. Rev. B: Condens. Matter Mater. Phys.*, 2008, **77**, 155402.
59 K. Park and M. R. Pederson, *Phys. Rev. B: Condens. Matter Mater. Phys.*, 2004, **70**, 054414.
60 L. Michalak, C. M. Canali and V. G. Benza, *Phys. Rev. Lett.*, 2006, **97**, 096804.
61 V. Meded, A. Bagrets, K. Fink, R. Chandrasekar, M. Ruben, F. Evers, A. Bernand-Mantel, J. S. Seldenthuis, A. Beukman and H. S. J. van der Zant, *Phys. Rev. B: Condens. Matter Mater. Phys.*, 2011, **83**, 245415.
62 F. Prins, M. Monrabal-Capilla, E. A. Osorio, E. Coronado and H. S. J. van der Zant, *Adv. Mater.*, 2011, **23**, 1545.
63 T. G. Gopakumar, F. Matino, H. Naggert, A. Bannwarth, F. Tuczek and R. Berndt, *Angew. Chem., Int. Ed.*, 2012, **51**, 6262.
64 D. Aravena and E. Ruiz, *J. Am. Chem. Soc.*, 2012, **134**, 777.
65 N. Baadji and S. Sanvito, *Phys. Rev. Lett.*, 2012, **108**, 217201.
66 A. Droghetti and S. Sanvito, *Phys. Rev. Lett.*, 2011, **107**, 047201.
67 A. Calzolari, Y. F. Chen, G. F. Lewis, D. B. Dougherty, D. Shultz and M. B. Nardelli, *J. Phys. Chem. B*, 2012, **116**, 13141.
68 A. Zunger, J. P. Perdew and G. L. Oliver, *Solid State Commun.*, 1980, **34**, 933.
69 J. P. Perdew, E. R. Mcmullen and A. Zunger, *Phys. Rev. A: At., Mol., Opt. Phys.*, 1981, **23**, 2785.
70 J. P. Perdew and A. Zunger, *Phys. Rev. B: Condens. Matter Mater. Phys.*, 1981, **23**, 5048.
71 A. Ruzsinszky, J. P. Perdew, G. I. Csonka, G. E. Scuseria and O. A. Vydrov, *Phys. Rev. A: At., Mol., Opt. Phys.*, 2008, **77**, 184109.
72 A. Ruzsinszky, J. P. Perdew, G. I. Csonka, O. A. Vydrov and G. E. Scuseria, *J. Chem. Phys.*, 2006, **125**, 194112.
73 M. R. Pederson and J. P. Perdew, *Self-Interaction Correction in Density Functional Theory: The Road Less Traveled*, http://www.psi-k.org/newsletters/News_109/Highlight_109.pdf.